

Photoinduced Charge-Carrier Generation in Epitaxial MOF Thin Films: High Efficiency as a Result of an Indirect Electronic Band Gap?*

Jinxuan Liu,* Wencai Zhou, Jianxi Liu, Ian Howard, Goran Kilibarda, Sabine Schlabach, Damien Coupry, Matthew Addicoat, Satoru Yoneda, Yusuke Tsutsui, Tsuneaki Sakurai, Shu Seki, Zhengbang Wang, Peter Lindemann, Engelbert Redel, Thomas Heine, and Christof Wöll*

Abstract: For inorganic semiconductors crystalline order leads to a band structure which gives rise to drastic differences to the disordered material. An example is the presence of an indirect band gap. For organic semiconductors such effects are typically not considered, since the bands are normally flat, and the band-gap therefore is direct. Herein we show results from electronic structure calculations demonstrating that ordered arrays of porphyrins reveal a small dispersion of occupied and unoccupied bands leading to the formation of a small indirect band gap. We demonstrate herein that such ordered structures can be fabricated by liquid-phase epitaxy and that the corresponding crystalline organic semiconductors exhibit superior photophysical properties, including large charge-carrier mobility and an unusually large charge-carrier generation efficiency. We have fabricated a prototype organic photovoltaic device based on this novel material exhibiting a remarkable efficiency.

The demand for devices converting solar energy into electrical power has been growing with accelerating speed over the past years. Although today the highest conversion efficiencies are achieved with photovoltaic devices based on inorganic semiconductors, such as silicon, the use of organic materials offers an interesting, less-expensive alternative.

Although the first organic photovoltaic (OPV) devices were reported about 50 years ago,^[1] progress in improving efficiency and stability is slow since the search for organic molecules that are suited to be an active material in OPV

devices is to a large extent still dominated by empirical approaches. Herein, we introduce a highly ordered system with an exactly known structure allowing the device characteristics to be understood on the basis of high-level electronic structure calculations. We provide evidence, that in our highly ordered systems an additional mechanism, the formation of indirect band gaps^[2] (Figure 1), comes into play which can substantially improve device performance. Indirect band gaps

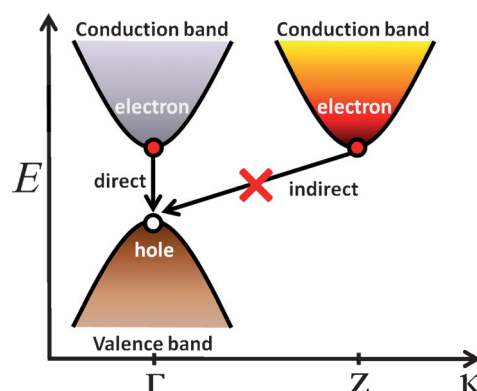


Figure 1. Schematic representations of recombination process of free electrons and holes in a solid with an indirect and direct band gap. The hole–electron recombination is not allowed in an indirect band-gap solid.^[2]

[*] Dr. J. Liu, W. Zhou, J. Liu, Dr. Z. Wang, P. Lindemann, Dr. E. Redel, Prof. Dr. C. Wöll
Institute of Functional Interfaces
Karlsruhe Institute of Technology
76344 Eggenstein-Leopoldshafen (Germany)
E-mail: jinxuan.liu@dlut.edu.cn
christof.woell@kit.edu

Dr. J. Liu
Institute of Artificial Photosynthesis, State Key Laboratory of Fine Chemicals, Dalian University of Technology (China)

Dr. I. Howard
Institute of Microstructure Technology
Karlsruhe Institute of Technology (Germany)
Dr. G. Kilibarda, Dr. S. Schlabach
Institute for Applied Materials
Karlsruhe Institute of Technology (Germany)

D. Coupry, Dr. M. Addicoat, Prof. T. Heine
Engineering and Science, Jacobs-University Bremen, Department of Physics and Earth Science, 28759 Bremen (Germany)
S. Yoneda, Y. Tsutsui, Dr. T. Sakurai, Prof. Dr. S. Seki
Department of Applied Chemistry, Graduate School of Engineering, Osaka University (Japan)

[**] We thank Mr. W. Guo, Mr. S. Heissler, Dr. M. Silverstre, Dr. H. Sezen, Dr. Rüdiger Berger, Dr. P. G. Weidler and Dr. H. Gliemann for help with the experiments and valuable discussions. Dr. A. Kuc is thanked for support in the band-structure calculations. Financial support by German DFG through SPP 1362 is gratefully acknowledged. W.Z., J.L., and Z.W. thank the Chinese Scholarship Council (CSC) for financial support. M.A. acknowledges financial support through the Marie S. Curie IIF program. Support from the KNMF Laboratory for Microscopy and Spectroscopy at KIT is acknowledged.

Supporting information for this article is available on the WWW under <http://dx.doi.org/10.1002/anie.201501862>.

support fast and highly efficient charge separation and strongly suppress charge-carrier recombination.

The importance of regular arrays of photoactive molecules for OPV performance is demonstrated by considering a class of biological molecules, porphyrins. In the natural systems, these light-harvesting molecules are typically stacked to yield extended columns through which the absorbed sunlight energy is transported in the form of excitons. Charge separation, that is, the dissociation of the exciton to yield an electron, e , and a hole, h , is achieved at a target chlorophyll pigment center.^[3]

In the past, a large amount of work has been devoted to preparing well-defined, thin porphyrin layers either by evaporation of porphyrin molecules on solid substrates, a very expensive method, or by self-assembly.^[4] Although especially in the self-assembly approach enormous progress has been achieved,^[5] the resulting systems are not highly ordered and not strictly crystalline.

Herein we present an unconventional approach based on confined self-assembly to fabricate crystalline porphyrin coatings employing a cheap, easily scalable technology. Using liquid-phase epitaxy (LPE) method, oriented, highly porous, crystalline, monolithic thin films are grown on a transparent and conductive substrate. The spray-based variant of this technique^[6] allows for fairly large substrate sizes (up to $10 \times 10 \text{ cm}^2$) and can be turned into a continuous process, thus providing a major advantage over, for example, spin-coating, where maximum size which is rather limited and for which a continuous coating is not possible.

The crystalline porphyrin solids fabricated using the LPE method correspond to a special type of metal-organic framework (MOF), a class of hybrid compounds which have received enormous attention in the past decades.^[7] Basically, MOFs are formed by attaching organic linkers to metal or metal-oxo nodes. In the present work we focus on a particular type of MOF referred to as “SURMOF 2” comprising so called paddle-wheel units which are stacked to yield an overall P4 symmetry.^[8] Whereas porphyrin-based MOFs have been studied previously,^[9] monolithic, homogenous films deposited on substrates which can act as electrodes in an OPV device have not yet been reported. Instead of the conventional solvothermal process yielding MOF powders,^[10] SURMOFs (surface-grafted MOFs) are grown in a layer-by-layer fashion on an appropriately functionalized substrate (Figure 2a). Because of the well-defined anchoring of the MOF-framework on the electrodes, SURMOFs offer huge promise for electrical applications of MOFs, for example, in the context of electrochemistry^[11] and electrically conducting thin films.^[12]

In the present study, we use conductive FTO (fluorine-doped tin oxide) substrates as the bottom electrode. An iodine/triiodine electrolyte (I^-/I_3^- in acetonitrile) was chosen as the top electrode (Figure 2b). This is a robust contacting strategy as mechanical or chemical (by reaction with vapor-deposited metal atoms) damage can be excluded.

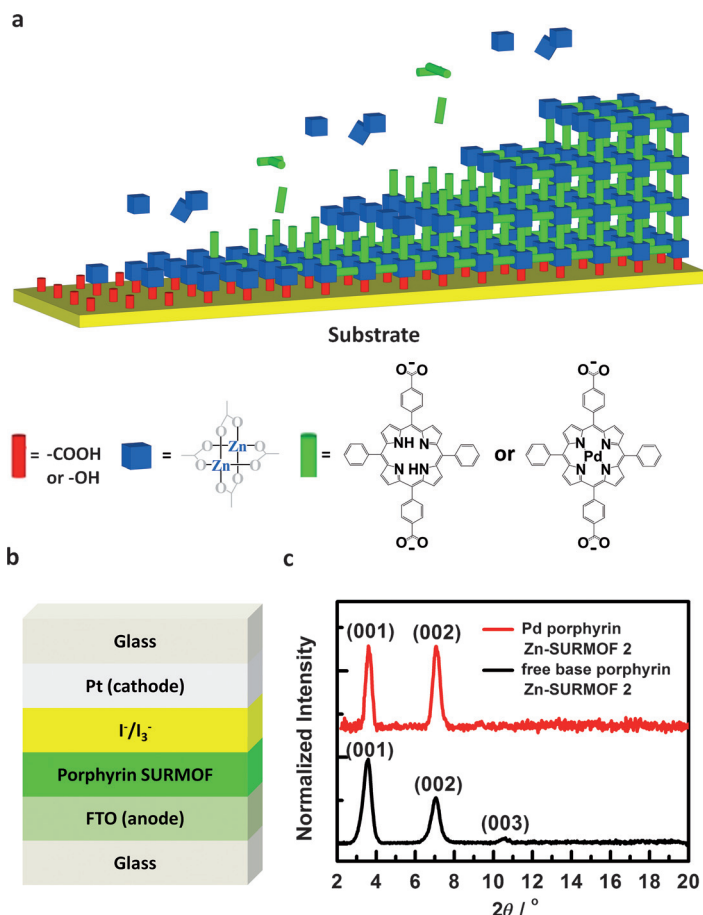


Figure 2. SURMOF preparation and characterization. a) Idealized schematic description of liquid-phase epitaxy deposition process on functionalized substrates in a layer-by-layer fashion with zinc acetate and free-base porphyrin and Pd porphyrin organic linkers. b) Architecture of porphyrin SURMOF-based photovoltaic device. c) Out of plane X-ray diffraction data of free-base porphyrin Zn-SURMOF 2 and Pd porphyrin Zn-SURMOF 2 grown on FTO glass substrates.

The X-ray diffraction (XRD) data shown in Figure 2c for a free-base porphyrin Zn-SURMOF 2 (thickness about 300 nm) show sharp and intense peaks revealing the presence of a highly oriented, well-ordered crystalline organic solid (Figure S1–S4 in the Supporting Information). Further characterizations using scanning electron microscopy (SEM), X-ray photoelectron spectroscopy (XPS), ultraviolet visible spectroscopy (UV/Vis), and IR spectroscopy (Figure S5–S12) confirm these findings.

The intrinsic charge-carrier transport property as well as carrier generation efficiency within the well-defined SURMOF thin layers were investigated by a flash-photolysis time-resolved microwave conductivity (FP-TRMC) system coupled with transient absorption spectroscopy (TAS). Both the free-base porphyrin Zn-SURMOFs 2 and Pd-porphyrin Zn-SURMOFs 2 showed typical transient conductivity ($\varphi\Sigma\mu$) upon photoexcitation at 355 nm (Figure S26). Along with that, they displayed transient absorption and photo-bleaching in their Soret band region (Figure S27), which indicates the photo-generation of porphyrin radical cations (holes). Importantly, the charge carrier generation efficiency (φ) amounted

to $\varphi = 9.5 \times 10^{-2}$ and 5.0×10^{-2} for the Pd and free-base systems, respectively. Such high efficiencies have not yet been reported for organic materials, the largest values reported to date for other MOFs materials^[13] or porphyrin-based covalent organic frameworks (COFs)^[14] amount to around 10^{-4} , almost three orders of magnitude smaller than the present value. In addition, since the kinetic profiles in FP-TRMC and TAS were well correlated (Figure S28), it was possible to determine the local-scale charge-carrier mobility for holes in the SURMOFs. The resulting values, $0.002 \text{ cm}^2 \text{ V}^{-1} \text{ s}^{-1}$ for Pd-porphyrin Zn-SURMOF 2 and $0.003\text{--}0.004 \text{ cm}^2 \text{ V}^{-1} \text{ s}^{-1}$ for free-base porphyrin Zn-SURMOF 2, are large compared to those reported for another MOF, MIL-125(Ti),^[15] with $\mu_h \approx 10^{-5} \text{ cm}^2 \text{ V}^{-1} \text{ s}^{-1}$, but slightly smaller than those reported for a tetrathiafulvalen-based MOF structure^[13a] ($0.2 \text{ cm}^2 \text{ V}^{-1} \text{ s}^{-1}$).

In a next step we have used this interesting porphyrin-based MOF material for the construction of a photovoltaic cell. In Figure 3 we show a current–voltage (I – V) curve recorded for a free-base porphyrin Zn-SURMOF 2 photovoltaic device under illumination with artificial sunlight.

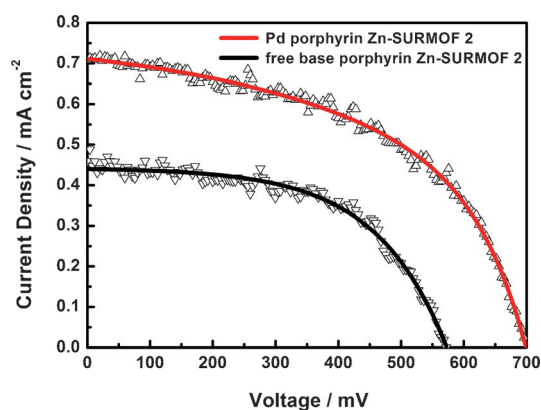


Figure 3. Photocurrent versus voltage (J – V) characteristics for free-base porphyrin Zn-SURMOF 2 and Pd porphyrin Zn-SURMOF 2 based photovoltaic device under illumination of AM 1.5 G simulated solar light (100 mW cm^{-2}) with liquid electrolyte (I^-/I_3^-) and active area 0.25 cm^2 .

An analysis of the data shown in Figure 3 yields an open-circuit voltage of 0.57 V , a short-circuit current density of 0.45 mA cm^{-2} , a fill factor of 0.55 and an efficiency of 0.2% . Using the simplest modification strategy, adding a Pd atom into the center of this polycyclic compound (Figure 2), already more than doubles the efficiency to yield 0.45% , see Figure 3 (open-circuit voltage of 0.7 V , short circuit current density of 0.71 mA cm^{-2} , fill factor of 0.65). We attribute the remarkably high OPV-performance for the Pd-system to the high photocarrier generation efficiency of this MOF-material (see above).

For a single-component OPV simply sandwiched between two electrodes such a solar cell performance is rather impressive. The corresponding photoresistivity data (Figure S13,S14) suggest that the exciton diffusion length in the porphyrin-based SURMOFs must be on the order of several 100 nm . The observation of such large exciton diffusion

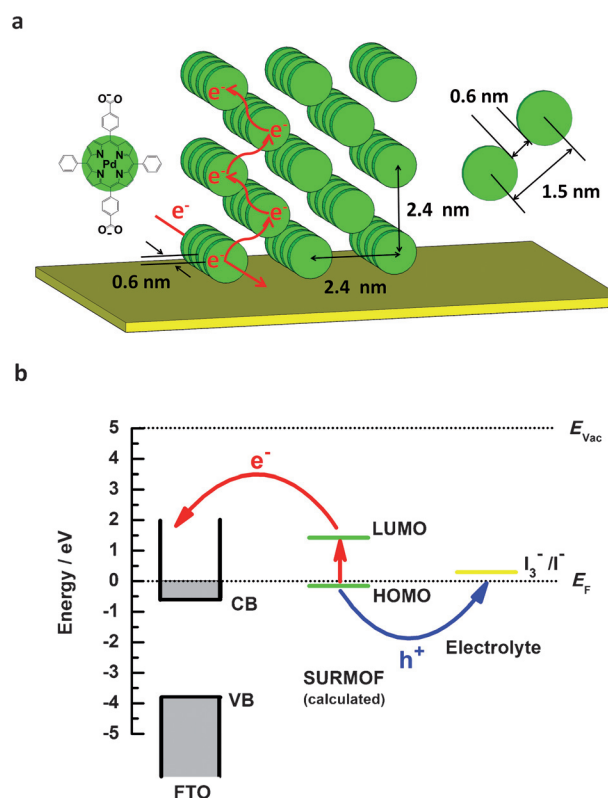


Figure 4. a) Nematic stacking of porphyrin units in porphyrin SURMOFs, the paddle-wheels are omitted for the purpose of clarity. b) Schematic description of photon absorption and exciton separation process in a porphyrin SURMOF photovoltaic device. The energy value of iodine/triiodine electrolyte in acetonitrile was taken from Ref. [17]. E_F = Fermi level.

lengths on the order of 20 nm has already been reported earlier for quasi-periodic nematic packings of the porphyrin units^[4] (Figure 4a).

The successful operation of our porphyrin SURMOF-based photovoltaic device can be rationalized by considering the energy-level diagram which shows the positions of the F:SnO_2 substrate flatband^[16] and that of the porphyrin SURMOFs MOs. On the basis of this existing knowledge and our calculations (see Supporting Information) we propose that the electrons are injected from the MOF porphyrin-ligands into the FTO substrate, (Figure 4b).

The photoluminescence and transient absorption data (Figure S15,S16) reveal a pronounced decrease of singlet exciton lifetime relative to the corresponding porphyrins in solution and suggest a fast and high-yield formation of long-lived states by converting the singlet exciton into triplet states.

The presence of an organic solid with known, strictly periodic structure now allows for a meaningful comparison to the results of high-level electronic structure calculations. First, the atomistic MOF structure was obtained from force field calculations. Then, the porphyrin electronic structure and light absorption were computed. In fact, the HOMO–LUMO energy difference of a saturated, single porphyrin molecule is essentially identical to the band gap at the Γ point of the periodic structure. For free-base porphyrin Zn-SURMOF 2, a band gap of 1.58 eV (DFTB level, DFTB = density-func-

tional based tight-binding) nearly coincides with the 1.60 eV HOMO–LUMO gap of the saturated single porphyrin molecule. The value of the saturated single porphyrin molecule can be compared with higher level theory (TD-DFT), which gives 1.51 eV for the same system. Introduction of metal centers increases the band gap to 1.94 eV (Pd porphyrin Zn-SURMOF 2) and 1.88 eV (Zn porphyrin Zn-SURMOF 2).

Next, we investigated the GGA-DFT band structure of Pd porphyrin Zn-SURMOF 2, the system with the highest efficiency in this study (Figure 5). At first sight the band structure appears to comply with the expectation that the bands are essentially flat.

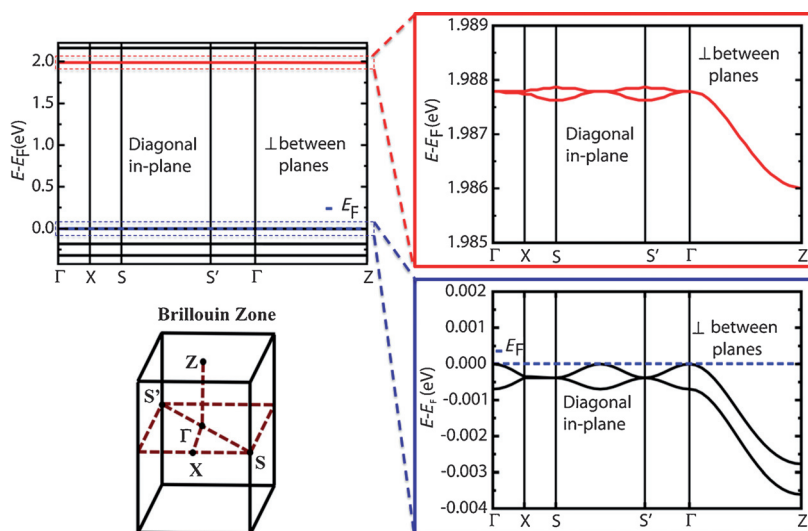


Figure 5. Band structure of Pd porphyrin Zn-SURMOF 2. Calculated band structure at the PBE level, the high-symmetry k points are indicated in the sketch of the Brillouin zone (left). The magnified two frontier bands of the conduction and valence bands are given on the right. The Fermi level is defined as the valence-band maximum.

A closer inspection, however, reveals a small but distinct dispersion of about 3 meV for both valence and conduction bands. The strongest dispersion is seen in the Γ -Z direction, perpendicular to the paddle-wheel-planes, along the columns of the stacked porphyrin disks. This observation reveals that the intermolecular overlap is strongest along the columns. The dispersion allows the effective masses of the charge carriers to be estimated, giving $4.5m_e$ (holes) and $9.6m_e$ (electrons). These values are an order of magnitude higher than in traditional semiconductors such as silicon, but appreciable in comparison with other organic materials. Importantly, the minimum in the conduction band (CB) is at the Z-point, whereas the maximum of the valence band (VB) is at the Γ -point. The SURMOF 2 structure thus has to be classified as an indirect band-gap semiconductor.^[18] The energy gain from the band dispersion is only on the order of 5 meV and thus certainly not sufficient for electron–hole separation. However, once electrons and holes are relaxed, direct electron–hole recombination is suppressed unlike in direct band-gap systems. Good carrier mobility along with suppressed recombination is consistent with the impressive behavior of the MOF-based OPV realized.

To our knowledge, indirect band gaps have not yet been realized in connection with organic semiconductors and also only in very few cases has the possibility of this feature been discussed.^[2] The fact that the indirect band-gap for the Pd porphyrin Zn-SURMOF 2 is substantially larger than for the free-base porphyrin Zn-SURMOF 2 is fully consistent with the substantially better OPV performance of the metal porphyrin system.

A calculation of the exciton lifetime which would allow an estimation of the exciton diffusion length is beyond the scope of the present work. We feel that we can safely link the experimentally observed, unexpected high performance of the MOF-based OPV devices to the fact that the porphyrin-MOFs are indirect band-gap semiconductors.

Since the crystalline lattices fabricated herein are highly porous we see the chance of achieving much higher performances, in particular a better charge separation, in the future by loading the pores within the frameworks with other, charge-donating or charge-accepting molecules. Photoactive molecules, such as fullerenes or Eu-based luminescent molecules,^[19] have already been successfully loaded into MOF frameworks. In addition, the liquid-phase epitaxy process used to fabricate the SURMOFs is well suited for heteroepitaxy,^[20] so that the stacking of different SURMOF layers with porphyrin-based ligands modified to absorb in different spectral areas becomes possible. Finally, because of their favorable mechanical properties,^[21] MOF thin films are also suitable for the fabrication of flexible devices. Further developments will profit from the possibility to apply high-level theory for these highly ordered systems.

Experimental Section

The porphyrin SURMOFs were deposited directly onto various substrates using a high-throughput automated spray system. The samples were comprehensively characterized with XRD, IR, XPS, SEM, Fluorescence spectroscopy, CV, UV/Vis, QCM, TAS, and FP-TRMC. For the photovoltaic devices porphyrin SURMOFs were grown on FTO anodes, Pt-coated glass together with I^-/I_3^- electrolyte was used as anode. Full details of substrates treatment, porphyrin SURMOF preparation, device fabrication, characterization techniques and force field and DFT calculations are available in the Supporting Information.

Keywords: metal–organic frameworks · semiconductors · photocarrier mobility · photovoltaic device · porphyrin

How to cite: *Angew. Chem. Int. Ed.* **2015**, *54*, 7441–7445
Angew. Chem. **2015**, *127*, 7549–7553

- [1] L. T. Dou, J. B. You, Z. R. Hong, Z. Xu, G. Li, R. A. Street, Y. Yang, *Adv. Mater.* **2013**, *25*, 6642–6671.
- [2] D.-K. Seo, R. Hoffmann, *Theor. Chem. Acc.* **1999**, *102*, 23–32.
- [3] H. Zhou, X. F. Li, T. X. Fan, F. E. Osterloh, J. Ding, E. M. Sabio, D. Zhang, Q. X. Guo, *Adv. Mater.* **2010**, *22*, 951–956.

- [4] A. Huijser, B. M. J. M. Suijkerbuijk, R. J. M. K. Gebbink, T. J. Savenije, L. D. A. Siebbeles, *J. Am. Chem. Soc.* **2008**, *130*, 2485–2492.
- [5] a) K. E. Martin, Z. C. Wang, T. Busani, R. M. Garcia, Z. Chen, Y. B. Jiang, Y. J. Song, J. L. Jacobsen, T. T. Vu, N. E. Schore, B. S. Swartzentruber, C. J. Medforth, J. A. Shelnutt, *J. Am. Chem. Soc.* **2010**, *132*, 8194–8201; b) K. K. Ng, J. F. Lovell, A. Vedadi, T. Hajian, G. Zheng, *ACS Nano* **2013**, *7*, 3484–3490; c) T. Higashino, H. Imahori, *Dalton Trans.* **2015**, *44*, 448–463.
- [6] H. K. Arslan, O. Shekhah, J. Wohlgemuth, M. Franzreb, R. A. Fischer, C. Wöll, *Adv. Funct. Mater.* **2011**, *21*, 4228–4231.
- [7] a) J. Lee, O. K. Farha, J. Roberts, K. A. Scheidt, S. T. Nguyen, J. T. Hupp, *Chem. Soc. Rev.* **2009**, *38*, 1450–1459; b) O. Shekhah, J. Liu, R. A. Fischer, C. Wöll, *Chem. Soc. Rev.* **2011**, *40*, 1081–1106; c) L. E. Kreno, K. Leong, O. K. Farha, M. Allendorf, R. P. Van Duyne, J. T. Hupp, *Chem. Rev.* **2012**, *112*, 1105–1124; d) H. Furukawa, K. E. Cordova, M. O’Keeffe, O. M. Yaghi, *Science* **2013**, *341*, 974–986; e) P. Ramaswamy, N. E. Wong, G. K. H. Shimizu, *Chem. Soc. Rev.* **2014**, *43*, 5913–5932.
- [8] J. X. Liu, B. Lukose, O. Shekhah, H. K. Arslan, P. Weidler, H. Gliemann, S. Brase, S. Grosjean, A. Godt, X. L. Feng, K. Mullen, I. B. Magdau, T. Heine, C. Wöll, *Sci. Rep.* **2012**, *2*, 1–5.
- [9] a) R. Makiura, S. Motoyama, Y. Umemura, H. Yamanaka, O. Sakata, H. Kitagawa, *Nat. Mater.* **2010**, *9*, 565–571; b) S. Motoyama, R. Makiura, O. Sakata, H. Kitagawa, *J. Am. Chem. Soc.* **2011**, *133*, 5640–5643; c) D. W. Feng, W. C. Chung, Z. W. Wei, Z. Y. Gu, H. L. Jiang, Y. P. Chen, D. J. Darensbourg, H. C. Zhou, *J. Am. Chem. Soc.* **2013**, *135*, 17105–17110; d) M. C. So, S. Jin, H.-J. Son, G. P. Wiederrecht, O. K. Farha, J. T. Hupp, *J. Am. Chem. Soc.* **2013**, *135*, 15698–15701; e) H. J. Son, S. Y. Jin, S. Patwardhan, S. J. Wezenberg, N. C. Jeong, M. So, C. E. Wilmer, A. A. Sarjeant, G. C. Schatz, R. Q. Snurr, O. K. Farha, G. P. Wiederrecht, J. T. Hupp, *J. Am. Chem. Soc.* **2013**, *135*, 862–869.
- [10] X. M. Chen, M. L. Tong, *Acc. Chem. Res.* **2007**, *40*, 162–170.
- [11] A. Dragässer, O. Shekhah, O. Zybaylo, C. Shen, M. Buck, C. Wöll, D. Schlottwein, *Chem. Commun.* **2012**, *48*, 663–665.
- [12] A. A. Talin, A. Centrone, A. C. Ford, M. E. Foster, V. Stavila, P. Haney, R. A. Kinney, V. Szalai, F. El Gabaly, H. P. Yoon, F. Leonard, M. D. Allendorf, *Science* **2014**, *343*, 66–69.
- [13] a) T. C. Narayan, T. Miyakai, S. Seki, M. Dinca, *J. Am. Chem. Soc.* **2012**, *134*, 12932–12935; b) L. Sun, T. Miyakai, S. Seki, M. Dinca, *J. Am. Chem. Soc.* **2013**, *135*, 8185–8188.
- [14] a) A. Kira, T. Umeyama, Y. Matano, K. Yoshida, S. Isoda, J. K. Park, D. Kim, H. Imahori, *J. Am. Chem. Soc.* **2009**, *131*, 3198–3200; b) X. Feng, L. L. Liu, Y. Honsho, A. Saeki, S. Seki, S. Irle, Y. P. Dong, A. Nagai, D. L. Jiang, *Angew. Chem. Int. Ed.* **2012**, *51*, 2618–2622; *Angew. Chem.* **2012**, *124*, 2672–2676.
- [15] M. A. Nasalevich, M. G. Goesten, T. J. Savenije, F. Kapteijn, J. Gascon, *Chem. Commun.* **2013**, *49*, 10575–10577.
- [16] a) M. Turrión, J. Bisquert, P. Salvador, *J. Phys. Chem. B* **2003**, *107*, 9397–9403; b) A. Klein, C. Korber, A. Wachau, F. Sauberlich, Y. Gassenbauer, S. P. Harvey, D. E. Proffit, T. O. Mason, *Materials* **2010**, *3*, 4892–4914.
- [17] G. Boschloo, A. Hagfeldt, *Acc. Chem. Res.* **2009**, *42*, 1819–1826.
- [18] P. Hofmann, *Solid State Physics: An Introduction*, Wiley-VCH, Berlin, **2008**.
- [19] H. C. Streit, M. Adlung, O. Shekhah, X. Stammer, H. K. Arslan, O. Zybaylo, T. Ladnorg, H. Gliemann, M. Franzreb, C. Wöll, C. Wickleder, *ChemPhysChem* **2012**, *13*, 2699–2702.
- [20] Z. B. Wang, J. X. Liu, B. Lukose, Z. G. Gu, P. G. Weidler, H. Gliemann, T. Heine, C. Wöll, *Nano Lett.* **2014**, *14*, 1526–1529.
- [21] S. Bundschuh, O. Kraft, H. K. Arslan, H. Gliemann, P. G. Weidler, C. Wöll, *Appl. Phys. Lett.* **2012**, *101*, 101910–101913.

Received: February 26, 2015

Published online: May 8, 2015